OPEN

Ischemic Preconditioning Blunts Loss of Knee Extensor Torque Complexity with Fatigue

JAMIE PETHICK, CHARLOTTE CASSELTON, SAMANTHA L. WINTER, and MARK BURNLEY

Endurance Research Group, School of Sport and Exercise Sciences, University of Kent, Kent, UNITED KINGDOM

ABSTRACT

PETHICK, J., C. CASSELTON, S. L. WINTER, and M. BURNLEY. Ischemic Preconditioning Blunts Loss of Knee Extensor Torque Complexity with Fatigue. *Med. Sci. Sports Exerc.*, Vol. 53, No. 2, pp. 306–315, 2021. **Introduction:** Neuromuscular fatigue reduces the temporal structure, or complexity, of muscle torque output, purportedly through an effect on motor unit behavior. Ischemic preconditioning (IPC), an emerging ergogenic aid, has been demonstrated to have a potent effect on muscular output and endurance. We therefore tested the hypothesis that IPC would attenuate the fatigue-induced loss of muscle torque complexity. **Methods:** Ten healthy participants (6 males/4 females) performed intermittent isometric knee extension contractions (6 s contraction, 4 s rest) to task failure at 40% maximal voluntary contraction. Contractions were preceded by either IPC (three bouts of 5 min proximal thigh occlusion at 225 mm Hg, interspersed with 5 min rest) or SHAM (as IPC, but occlusion at only 20 mm Hg) treatments. Torque and EMG signals were sampled continuously. Complexity and fractal scaling were quantified using approximate entropy (ApEn) and the detrended fluctuation analysis (DFA) α scaling exponent. Muscle oxygen consumption ($m\dot{V}O_2$) was determined using near-infrared spectroscopy. **Results:** IPC increased time to task failure by 43% ± 13% (mean ± SEM, $P = 0.047$). Complexity decreased in both trials (decreased ApEn, increased DFA α; both $P < 0.001$), although the rate of decrease was significantly lower after IPC (ApEn, −0.2 ± 0.1 vs –0.4 ± 0.1, $P = 0.013$; DFA α, 0.2 ± 0.1 vs 0.3 ± 0.1, $P = 0.037$). Similarly, the rates of increase in EMG amplitude ($P = 0.022$) and $m\dot{V}O_2$ ($P = 0.043$) were significantly slower after IPC. **Conclusion:** These results suggest that the ergogenic effect of IPC observed here is of neural origin and accounts for the slowing of the rates of change in torque complexity, EMG amplitude, and $m\dot{V}O_2$ as fatigue develops. **Key Words:** EXERCISE, ERGOGENIC AIDS, MUSCULAR ENDURANCE, NONLINEAR DYNAMICS, MUSCLE ACTIVITY

BASIC SCIENCES

The optimal pattern of force (or torque) production is often presumed to be one that is smooth and accurate, relative to the task demands. However, even in health, muscular output fluctuates in a seemingly random fashion around the required target (1), with perturbations such as neuromuscular fatigue (2) and aging (3) exacerbating these fluctuations. It was long thought that such fluctuations were unwanted system noise or a reflection of underlying pathology (4), although it is now being increasingly recognized that they may provide significant insight into motor control (5,6). Over the past 20 yr, it has become evident that the fluctuations in muscle torque output are not simply random noise; rather, they possess a statistically irregular temporal structure, or "complexity" (1). Measures of complexity quantify the degree of signal regularity (e.g., approximate entropy [ApEn] [7]) and identify the presence of long-range fractal correlations (e.g., detrended fluctuation analysis [DFA] [8]). The presence of complexity in muscular output is thought to reflect the adaptability of the neuromuscular system and the ability to modulate motor output rapidly and accurately in response to task demands (5).

Any loss of complexity in muscle torque output is indicative of neuromuscular system dysfunction and reflects a decrement in motor control, which could have important implications for task performance (5,9). A loss of muscle torque complexity has been repeatedly observed with neuromuscular fatigue, occurring during both maximal and submaximal intermittent isometric contractions (6,9–11). Although the mechanism(s) underpinning this loss of complexity is unclear, we recently showed that caffeine ingestion delays task failure and slows the fatigue-induced loss of muscle torque complexity, concomitant to attenuation of the loss of maximum torque generating capacity and the development of central fatigue (12). Indeed, the loss of muscle torque complexity appears to be tightly coupled to the fatigue process, with complexity declining in tandem with the loss of torque generating capacity (12) and increase in muscle oxygen consumption ($m\dot{V}O_2$ [11]). Interventions that delay task failure and slow the neuromuscular

Address for correspondence: Mark Burnley, Ph.D., School of Sport and Exercise Sciences, University of Kent, The Medway Building, Chatham Maritime, Kent ME4 4AG, United Kingdom; E-mail: m.burnley@kent.ac.uk.
Submitted for publication May 2020.
Accepted for publication July 2020.

0195-9131/20/5302-0306/0
MEDICINE & SCIENCE IN SPORTS & EXERCISE®

DOI: 10.1249/MSS.0000000000002475

fatigue process should therefore be associated with an attenuated loss of muscle torque complexity (12). Moreover, such interventions should also provide further insight into the mechanistic basis of the fatigue-induced loss of complexity.

Ischemic preconditioning (IPC) is a noninvasive technique, originally conceived as a cardioprotective intervention, that consists of repeated cycles of brief ischemia followed by reperfusion (13). Since its first use in a sporting context as an ergogenic aid (14), IPC has been demonstrated to improve endurance in a variety of exercise modalities (15,16), including isometric contractions (17,18). Nevertheless, the mechanisms by which IPC exerts this ergogenic effect are complex and remain to be fully elucidated. Early findings suggested that IPC could serve to maintain oxygen supply and energy substrates to muscle, potentially through an effect on vascular or endothelial function (13,14). However, recent research of both clinical (19) and sporting (20) nature has suggested that neural mechanisms mediate the beneficial effects of IPC.

IPC has multiple positive effects on motor output, including increasing maximal force generation (21) and delaying task failure and neuromuscular fatigue (17,18). These results suggest that neural adjustments may in part account for the effect of IPC on exercise tolerance (22). Studies in anesthetized and electrically stimulated cats (23) and exercising humans (22,24) have demonstrated that IPC results in greater EMG activity and increased motor unit recruitment during maximal contractions and a decreased motor unit recruitment threshold during submaximal contractions (22). These findings are consistent with increased excitability of the motoneuron pool (25). We have previously argued that the fatigue-induced loss of muscle torque complexity must be related to factors directly affecting the motor unit pool (6), and indeed our previous data suggest that caffeine's ergogenic effect on muscle torque complexity was mediated by a greater ability to excite the motor unit pool in the face of developing fatigue (12).

IPC has been hypothesized to exert its ergogenic effect centrally through the stimulation of metabolite-sensitive group III and group IV muscle afferents, which in turn engage brainstem centers to release excitatory neuromodulators, such as serotonin and noradrenaline (13,26). An IPC-mediated increase in motoneuron excitability during fatiguing submaximal contractions should maintain central drive to the motoneuron pool (i.e., reduce the rate of central fatigue development). This, in turn, should delay the reduction in force generating capacity and delay the consequent rise in EMG amplitude characteristic of neuromuscular fatigue (27). If changes in muscle torque complexity are directly related to motor unit recruitment and discharge adjustments in response to fatigue, then IPC should also slow the fatigue-induced loss of torque complexity (12). The purpose of the present study was therefore to investigate the effect of IPC on muscle torque complexity during subsequent fatiguing isometric contractions. We hypothesized that IPC would increase time to task failure and attenuate the rate of the fatigue-induced reduction in muscle torque complexity, quantified by a slower rate of decrease in ApEn and a slower rate of increase in the DFA α scaling exponent.

MATERIALS AND METHODS

Participants

Ten healthy participants (6 males, 4 females; mean ± SD: age = 25.9 ± 6.7 yr, height = 1.72 ± 0.10 m, weight = 69.3 ± 12.7 kg) provided written informed consent to participate in the study, which was approved by the ethics committee of the University of Kent and which adhered to the Declaration of Helsinki. Participants were instructed to arrive at the laboratory in a rested state (having performed no strenuous exercise in the preceding 24 h) and to have consumed neither any food nor any caffeinated beverages in the 3 h before arrival. Participants attended the laboratory at the same time of day (±2 h) during each visit.

Experimental Design

Participants were required to visit the laboratory on three occasions over a 2- to 3-wk period, with a minimum of 72 h separating each visit. During their first visit, participants were familiarized with all testing equipment and procedures, and the settings for the dynamometer and femoral nerve stimulation were recorded. During the next two visits, participants performed, in a randomized order, a series of intermittent isometric knee extension contractions to task failure preceded by either an IPC or a sham treatment (SHAM). To minimize any placebo effect or bias, participants were told that the purpose of the study was to compare the impact of two different cuff pressures, both of which could potentially alter performance (21). In each trial, torque output was sampled continuously to allow the quantification of complexity, muscle activity was measured using the vastus lateralis EMG, $m\dot{V}O_2$ was measured using near-infrared spectroscopy (NIRS), and maximal voluntary contractions (MVC) with supramaximal femoral nerve stimulation were used to quantify global, central and peripheral fatigue.

Dynamometry

During all visits, participants were seated in the chair of a Cybex isokinetic dynamometer (HUMAC Norm; CSMi, Lawrence, MA), initialized and calibrated according to the manufacturer's instructions. Participants sat with relative hip and knee angles of 85° and 90°, respectively, with full extension being 0°. Their right leg was attached to the lever arm of the dynamometer, and the seating position was adjusted to ensure that the lateral epicondyle of the femur was in line with the axis of rotation of the lever arm. The lower leg was securely attached to the lever arm above the malleoli with a padded Velcro strap. Straps secured firmly across the waist and shoulders prevented any extraneous movement and the use of the hip extensors during the isometric contractions. The seating position was recorded during the familiarization and replicated during each subsequent visit.

EMG

The EMG of the vastus lateralis was sampled using Ag/AgCl electrodes (32 × 32 mm; Nessler Medizintechnik, Innsbruck, Austria). Before attachment of the electrodes, the skin of the

participants was shaved, abraded, and cleaned with an alcohol swab over the belly of the muscle to reduce impedance. The electrodes were placed on the prepared skin over the belly of the muscle, parallel to the alignment of the muscle fibers. A reference electrode was placed on prepared skin medial to the tibial tuberosity. Care was taken to ensure that the electrode locations were identical between sessions. The raw EMG signals were sampled at 1 kHz, amplified (gain 1000; Biopac MP150; Biopac Systems Inc., Goleta, CA), and band-pass filtered (10–500 Hz; Biopac MP150; Biopac Systems Inc.).

Femoral Nerve Stimulation

The electrical stimulation of the femoral nerve was used to assess neuromuscular fatigue processes, as described previously by Pethick et al. (6). The anode, a carbon rubber electrode with adhesive gel (100 × 50 mm; Phoenix Healthcare Products Ltd., Nottingham, UK), was placed lateral to the ischial tuberosity, on the posterior aspect of the leg. The position of the cathode was located using a motor point pen (Compex; DJO Global, Guildford, UK) and based on the location in the femoral triangle giving the largest twitch and greatest peak-to-peak amplitude of the compound muscle action potential (M-wave) after a single stimulation at 100 mA, using a constant-current, variable voltage stimulator (Digitimer DS7AH, Welwyn Garden City, UK). After the determination of the precise cathode location, an Ag/AgCl electrode (32 × 32 mm; Nessler Medizintechnik) was placed over that point.

The appropriate stimulator current was then established by incrementally increasing the current, in steps of 20 mA, until knee extensor torque and the M-wave response to single twitches had plateaued. This was verified with stimulation delivered during a contraction at 50% MVC to ensure that a maximal M-wave was also evident during an isometric contraction. The stimulator current was then increased to 130% of the current producing a maximal M-wave. In all subsequent trials, doublet stimulation (two 200-μs pulses with 10-ms interpulse interval) was used.

NIRS

The $m\dot{V}O_2$ of the vastus lateralis was obtained, as described by Pethick et al. (11), using a continuous-wave NIRS device (Oxymon Mk III; Artinis Medical Systems, Elst, Netherlands), calibrated according to the manufacturer's instructions before each trial. The NIRS device generated light at three wavelengths (905, 850, and 770 nm) corresponding to the absorption wavelengths of oxyhemoglobin (O_2Hb) and deoxyhemoglobin (HHb). An area at the level of the largest circumference of the vastus lateralis was shaved, abraded, and cleaned with an alcohol swab. The NIRS optode was then placed at this location and secured with Velcro straps and biadhesive tape, such that the optode could not move during contractions. A 13-cm-wide blood pressure cuff (Hokanson E20 cuff inflator; D.E. Hokanson Inc., Bellevue, WA) was placed proximal to the NIRS optode, at the top of the thigh, and was used to maintain blood volume under the optode during measurement. NIRS data were collected at 10 Hz. An ischemic calibration (performed at the end of each visit) eliminated any effect of adipose tissue thickness and scaled the NIRS signals according to the maximal physiological range (28).

Protocol

All visits followed a pattern of data acquisition similar to that which we have previously reported (6). Each visit began with the instrumentation of the participants and the establishment of the correct dynamometer seating position and supramaximal stimulation response. Participants then performed a series of brief (3 s) MVC to establish their maximum torque. These contractions were separated by a minimum of 60 s rest and continued until the peak torques in three consecutive contractions were within 5% of each other. Participants were given a countdown, followed by very strong verbal encouragement to maximize torque. The first MVC was used to establish the fresh (i.e., nonexercised) maximal EMG signal, against which the subsequent EMG signals were normalized (see Data analysis section). The second MVC and the third MVC were performed with femoral nerve stimulation delivered during the contraction and at rest after the contraction. The stimulation during the contraction was delivered during a plateau in maximal torque to test the maximality of the contractions and to provide the fresh voluntary activation, whereas the stimulation at rest was delivered 2 s after the contraction to establish the fresh potentiated doublet torque. All subsequent contractions with femoral nerve stimulation were conducted in this manner. Participants then rested for 10 min before undergoing either IPC or SHAM.

The IPC and the SHAM protocols were performed by means of rapid inflation of the blood pressure cuff, already positioned for the NIRS measurements, at the top of the thigh. In the IPC condition, the cuff was inflated to 225 Hg for three periods of 5 min, interspersed with 5-min periods of rest/reperfusion. In the SHAM condition, the cuff was inflated to only 20 mm Hg for three periods of 5 min, interspersed with 5-min periods of rest/reperfusion (21,29). After the completion of the IPC and SHAM protocols, participants rested for 20 min (29). They then performed an MVC, accompanied by femoral nerve stimulation, immediately before commencing the fatigue test.

Participants performed intermittent isometric knee extension contractions at 40% MVC. The target torque was based on the highest instantaneous torque recorded during the pretest MVC in the first experimental visit. The duty cycle for the contractions was 60%, with contractions held for 6 s and being followed by 4 s rest. Participants were instructed to match their instantaneous torque with a target bar superimposed on the display in front of them and were required to continue matching this torque for as much of the 6-s contraction as possible. The contractions continued until task failure, defined as the point at which the participants failed to reach the target torque on three consecutive contractions, despite strong verbal encouragement. Participants were not informed of the elapsed time during the trials but were informed of each "missed" contraction. At task failure, participants were instructed to immediately

produce an MVC, which was accompanied by femoral nerve stimulation.

Similar to the study of Pethick et al. (11), at the end of each minute of contractions (i.e., after every fifth contraction), $m\dot{V}O_2$ was assessed based on the decrease in muscle oxygenation which accompanies an arterial occlusion (28). The blood pressure cuff was rapidly inflated to 300 mm Hg for 5 s using a Hokanson AG101 (D.E. Hokanson Inc.), with $m\dot{V}O_2$ calculated using linear regression over the course of this occlusion. This measure of $m\dot{V}O_2$ was performed instead of a targeted contraction. $m\dot{V}O_2$ was also assessed immediately before the MVC performed at task failure. Five minutes after task failure, an ischemia/hyperemia calibration was performed to normalize the NIRS signals. The blood pressure cuff was inflated to 300 mm Hg for 5 min, with a plateau in the HHb signal being visually confirmed (28). This functionally, although not completely, deoxygenated the tissue under the optode (defined as 0% oxygenation), whereas the peak hyperemic response upon release of the cuff was assigned a value of 100% oxygenation.

Data Acquisition and Participant Interface

Data acquisition was performed in a similar manner as described by Pethick et al. (11). The isokinetic dynamometer, stimulator, and EMG were connected via BNC cables to a Biopac MP150 (Biopac Systems Inc.) and a CED Micro 1401-3 (Cambridge Electronic Design, Cambridge, UK) interfaced with a personal computer. These data were sampled at 1 kHz and collected in Spike2 (Version 7; Cambridge Electronic Design). The NIRS data were sampled at 10 Hz and collected in Oxysoft (Artinis Medical Systems).

A chart containing the instantaneous torque was projected onto a screen placed ~1 m in front of the participant. A scale consisting of a thin line (1 mm thick) was superimposed on the torque chart and acted as a target, so that participants were able to match their instantaneous torque output to the target torque during each visit.

Data Analysis

All data were analyzed using code written in MATLAB R2017a (The MathWorks, Natick, MA). The data analysis focused on four specific areas: 1) basic measures of torque and EMG, 2) measures of central and peripheral fatigue, 3) the variability and complexity of torque output, and 4) measures of $m\dot{V}O_2$.

Torque and EMG. The mean and the peak torque for each contraction in both trials were determined. The mean torque was calculated based on the steadiest 5 s of each contraction, with MATLAB code identifying the 5 s of each contraction with the lowest SD. The point of task failure was determined similar to the study of Pethick et al. (6). The mean torque produced during the first five contractions was calculated, with task failure deemed to occur when the mean torque recorded during three consecutive contractions was more than 5 N·m below the mean torque of the first five contractions, with the first of these contractions being considered the point of task failure.

The EMG output from the vastus lateralis for each contraction was full-wave rectified during each 5-s window. The average rectified EMG (arEMG) was then calculated and normalized by expressing the arEMG as a fraction of the mean arEMG obtained during a 3-s MVC from the fresh muscle performed at the beginning of the trial.

Central and peripheral fatigue. Measures of central and peripheral fatigue were calculated based on the stimuli delivered during and after the MVC performed pretest and at task end/failure. Peripheral fatigue was evidenced by a fall in the potentiated doublet torque. Central fatigue was evidenced by a decline in voluntary activation, quantified using the twitch interpolation technique (30):

$$\text{voluntary activation (\%)} = 1 - (\text{superimposed doublet}/\text{resting doublet}) \times 100 \quad [1]$$

where the superimposed doublet was that measured during the contraction of interest and the potentiated doublet was measured at rest 2 s after that contraction.

Variability and complexity. All measures of variability and complexity were calculated using the steadiest 5 s of each contraction, identified by MATLAB as the 5 s containing the lowest SD. The amount of variability in the torque output of each contraction was measured using the SD, which provides a measure of the absolute amount of variability in a time series, and coefficient of variation (CV), which provides a measure of the amount of variability in a time series normalized to the mean of the time series.

The temporal structure, or complexity, of torque output was examined using multiple time domain analyses, as recommended by Goldberger et al. (4). The regularity of torque output was determined using ApEn (7), and the temporal fractal scaling of torque was estimated using the DFA (8) α scaling exponent. The calculations of ApEn and DFA are detailed by Pethick et al. (6). In brief, ApEn was calculated with the template length m set at 2 and the tolerance r set at 10% of the SD of torque output, and DFA was calculated across time scales (57 boxes ranging from 1250 to 4 data points). In one participant in both the IPC and the SHAM conditions, a significant degree of crossover was identified in the log–log plot of fluctuation size versus box size (as shown by an $r < 0.95$). To account for this effect, a least squares linear regression was used to fit two lines to the plot, and two α exponents were quantified. The second of these (α_2, representing longer physiologic timescales) was used in the DFA α exponent analysis (11).

$m\dot{V}O_2$. $m\dot{V}O_2$ was determined as described by Ryan et al. (28). $m\dot{V}O_2$ was calculated as the slope of the change in O_2Hb and HHb during arterial occlusion using simple linear regression. The $m\dot{V}O_2$ measurements were based on the 5-s arterial occlusions (50 data points) at the end of each minute of exercise.

The NIRS data were corrected for blood volume changes as described by Ryan et al. (28), using custom-written MATLAB

TABLE 1. Effects of IPC and SHAM on voluntary torque and electrically elicited muscle contractile properties.

	SHAM		IPC	
Parameter	Pre	Post	Pre	Post
MVC, N·m	248.1 ± 26.6	228.6 ± 24.7*	249.1 ± 24.7	233.9 ± 24.2*
Doublet, N·m	91.7 ± 9.8	89.6 ± 10.1	90.5 ± 10.3	86.5 ± 8.8
VA, %	92.4 ± 0.9	90.0 ± 5.2	92.7 ± 1.6	90.4 ± 1.6

Values are presented as mean ± SEM.
*Significantly different from Pre.
VA, voluntary activation.

code. A blood volume correction factor (β) was calculated for each data point during the arterial occlusions:

$$\beta(t) = \frac{|O_2Hb(t)|}{(|O_2Hb(t)| + |HHb(t)|)} \quad [2]$$

where β is the blood volume correction factor, t is time, O_2Hb is the oxygenated hemoglobin/myoglobin signal, and HHb is the deoxygenated hemoglobin/myoglobin signal. Each data point was corrected using its corresponding β according to equations 3 and 4:

$$O_2Hb_c(t) = O_2Hb(t) - [tHb(t) \times (1 - \beta)] \quad [3]$$

$$HHb_c(t) = HHb(t) - [tHb(t) \times \beta] \quad [4]$$

where O_2Hb_c and HHb_c are the corrected oxygenated and deoxygenated hemoglobin/myoglobin signals, respectively; tHb is the blood volume signal from the NIRS device; β is the blood volume correction factor; and t is time. The raw O_2Hb signal in equation 3 is corrected by subtracting the proportion of the blood volume change attributed to O_2Hb, whereas the raw HHb signal in equation 4 is corrected by subtracting the proportion of blood volume change attributed to HHb.

Statistics

All data are presented as mean ± SEM. A two-way repeated-measures ANOVA was used to test for differences between conditions and time points, and for a condition–time interaction for MVC torque, arEMG, potentiated doublet torque, voluntary activation, variability, complexity, and $m\dot{V}O_2$. The arEMG, variability, complexity, and $m\dot{V}O_2$ measures were analyzed using means from the second minute (to account for the primary amplitude of the $\dot{V}O_2$ response [31]), isotime (the time point in the IPC condition equivalent to task failure in the SHAM condition [12]), and the final minute before task failure. When main effects were observed, Bonferroni-adjusted, paired-samples 95% confidence intervals (CI) were used to identify specific differences. Results were deemed statistically significant when $P < 0.05$.

RESULTS

Preliminary measures. The contractile properties of the knee extensors obtained 10 min before and 20 min after IPC/SHAM are shown in Table 1. These were intended to assess the effects of IPC in a rested state. Both IPC and SHAM resulted in a decrease in MVC torque (paired-samples 95% CI: IPC, −24.2 to −6.2 N·m; SHAM, −39.8 to −2.8 N·m). Neither IPC nor SHAM resulted in any significant change in either potentiated doublet torque or voluntary activation.

Time to task failure, MVC torque, and EMG. Example contractions from a representative participant are shown in Figure 1. IPC significantly increased time to task failure by 7.4 ± 3.2 min (95% CI = 0.1–14.7 min) or by 43% ± 13% (Table 2). Task failure occurred when participants were no longer able to achieve the target torque (100.3 ± 10.5 N·m), despite a maximal effort. Both conditions resulted in significant decreases in MVC torque ($F = 43.14$, $P < 0.001$), such that the mean MVC torque at task failure was not significantly different from the torque produced during the submaximal contractions. At task failure, there was no significant difference between the conditions for MVC torque (95% CI = −15.5 to 18.5 N·m). The rate of decrease in MVC torque was significantly attenuated in the IPC condition (IPC vs SHAM: −7.6 ± 2.0 vs −10.2 ± 2.8 N·m·min^{-1}; 95% CI = −5.2 to −0.4 N·m·min^{-1}; Table 2). The arEMG of

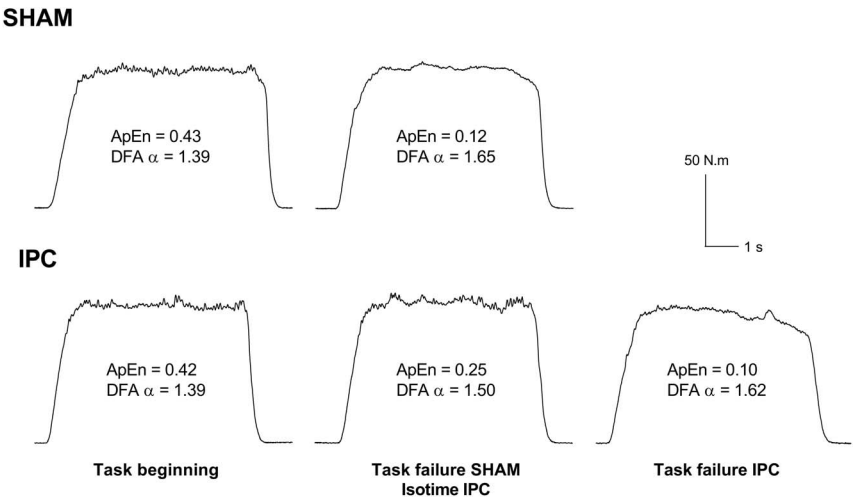

FIGURE 1—Raw torque output during contractions in the SHAM (*top panels*) and IPC (*bottom panels*) conditions from a representative participant.

TABLE 2. Voluntary torque, potentiated doublet torque, voluntary activation, EMG, and $m\dot{V}O_2$ responses during contractions in the IPC and SHAM conditions.

Parameter	SHAM	IPC
Time to task failure, min	17.3 ± 4.3	24.7 ± 6.2#
Global fatigue		
Preexercise MVC, N·m	228.6 ± 24.7	233.9 ± 24.2
Peak MVC at task failure, N·m	126.7 ± 16.0*	128.1 ± 17.4*
Mean MVC at task failure, N·m	104.8 ± 12.6	108.9 ± 14.8
$\Delta MVC/\Delta t$, N·m·min^{-1}	−10.2 ± 2.8	−7.6 ± 2.0#
Peripheral fatigue		
Preexercise doublet, N·m	89.6 ± 9.6	86.5 ± 8.4
Doublet at task failure, N·m	72.2 ± 10.0*	69.0 ± 8.0*
% Change at task failure	23.2 ± 5.0	24.4 ± 3.6
$\Delta doublet/\Delta t$, N·m·min^{-1}	−1.3 ± 0.2	−1.4 ± 0.6
Central fatigue		
Preexercise VA, %	90.0 ± 1.6	90.4 ± 1.5
VA at task failure, %	77.0 ± 3.0*	75.6 ± 3.6*
% Change at task failure	16. 7 ± 3.3	18.3 ± 4.2
$\Delta VA/\Delta t$, %·min^{-1}	−1.2 ± 0.4	−0.8 ± 0.2
Surface EMG		
arEMG at task beginning, %MVC	41.2 ± 3.1	37.0 ± 2.6
arEMG at isotime, %MVC	–	57.0 ± 3.6#
arEMG at task failure, %MVC	65.8 ± 5.2*	59.8 ± 4.8*
$\Delta arEMG/\Delta t$, %MVC·min^{-1}	2.4 ± 0.6	1.8 ± 0.5
$m\dot{V}O_2$		
$m\dot{V}O_2$ at task beginning, %·s^{-1}	2.3 ± 0.3	1.8 ± 0.3
$m\dot{V}O_2$ at isotime, %·s^{-1}	–	2.7 ± 0.3
$m\dot{V}O_2$ at task failure, %·s^{-1}	3.7 ± 0.4*	3.1 ± 0.3*
$\Delta m\dot{V}O_2/\Delta t$, %·s^{-1}	0.2 ± 0.05	0.1 ± 0.02#

Values are presented as mean ± SEM.
Symbols indicate a statistically significant difference compared with the following: *Preexercise value/value at task beginning (2 min into exercise, to account for primary amplitude of $\dot{V}O_2$ response). #SHAM. Isotime in the IPC condition is compared with task failure in the SHAM condition.
VA, voluntary activation; Δ, change; *t*, time.

the vastus lateralis increased over time in both conditions ($F = 43.41$, $P < 0.001$; Table 2; Fig. 2A). The rate of change in arEMG was significantly attenuated in the IPC condition (IPC vs SHAM: 1.8% ± 0.5% vs 2.4% ± 0.6%; 95% CI = −0.1% to −1.2%; Fig. 2C).

Peripheral and central fatigue. Both conditions resulted in significant reductions in potentiated doublet torque ($F = 53.94$, $P < 0.001$; Table 2), indicating the presence of peripheral fatigue. The values attained at task failure were not significantly different between the conditions (95% CI = −19.1 to 12.6 N·m). The rate of decrease in potentiated doublet torque was not significantly different between conditions (95% CI = –1.3 to 1.2 N·m·min^{-1}; Table 2). Both conditions also resulted in a significant decline in voluntary activation ($F = 20.43$, $P = 0.002$; Table 2), indicating the presence of central fatigue. The values attained at task failure were not significantly different between the conditions (95% CI = −6.8% to 4.0%). The rate of decrease in voluntary activation was not significantly different between conditions (95% CI = −0.2 to 0.9%·min^{-1}; Table 2).

$m\dot{V}O_2$. After 2 min of contractions, wherein a steady state should have been observed, both conditions resulted in a significant increase in $m\dot{V}O_2$ ($F = 17.23$, $P = 0.003$; Table 2; Fig. 2B). There were no significant differences between conditions after either 2 min of contractions (95% CI = −1.0 to 0.2%·s^{-1}) or at task failure (95% CI = −1.8 to 0.3%·s^{-1}). The rate of increase in $m\dot{V}O_2$ was significantly attenuated in the IPC condition (IPC vs SHAM: 0.08 ± 0.02 vs 0.16 ± 0.05%·s^{-1}; 95% CI = −0.2 to −0.003%·s^{-1}; Table 2; Fig. 2D).

Variability and complexity. Both conditions resulted in a significant increase in the amount of variability, as measured by the SD ($F = 29.45$, $P < 0.001$) and CV ($F = 43.19$, $P < 0.001$; Table 3). The values attained at task failure for the SD (95% CI = –0.4 to 0.5 N·m) and CV (95% CI = −1.9% to 3.2%) were not significantly different between conditions (Table 3). The rates of increase in the SD (95% CI = –0.2 to 0.2 N·m) and CV (95% CI = −0.2% to 0.2%) did not differ between conditions.

Complexity decreased as fatigue developed in both conditions, as measured by ApEn ($F = 102.99$, $P < 0.001$) and DFA α ($F = 29.64$, $P < 0.001$; Table 3; Fig. 3B and D). ApEn significantly decreased as the trials progressed, with the values at task failure being not significantly different between the conditions (95% CI = −0.05 to 0.09). However, at isotime in the IPC condition (the time point equivalent to task failure in the SHAM condition), ApEn remained significantly higher (IPC vs SHAM: 0.27 ± 0.04 vs 0.14 ± 0.02; 95% CI = 0.001–0.3; Fig. 3A). The rate of decrease in ApEn was significantly attenuated in the IPC condition (IPC vs SHAM: −0.02 ± 0.01 vs –0.04 ± 0.01; 95% CI = −0.003 to 0.02; Fig. 3C). DFA α significantly increased as the trials progressed, with the values at task failure being not significantly different between the conditions (95% CI = −0.08 to 0.02). The rate of increase in DFA α was significantly attenuated in the IPC condition (IPC vs SHAM: 0.02 ± 0.01 vs 0.03 ± 0.01; 95% CI = −0.02 to −0.007; Fig. 3D).

DISCUSSION

The major novel finding of the present study was that, consistent with our hypotheses, IPC delayed task failure and slowed the fatigue-induced loss of muscle torque complexity. These responses were accompanied by an attenuated rate of decrease in MVC torque and attenuated rates of increase in arEMG activity and $m\dot{V}O_2$. This investigation is the first to demonstrate that IPC positively influences muscle torque complexity and motor control, provides further evidence that the loss of muscle torque complexity is sensitive to the administration of ergogenic aids, and that this is tightly coupled to the neuromuscular fatigue process. Moreover, these results indicate that the effect of IPC, on both time to task failure and muscle torque complexity, may be mediated by an attenuated requirement for the recruitment of additional motor units.

Effect of IPC on muscle torque complexity and fatigue. It has recently been shown that IPC has a positive effect on motor output, increasing maximum force (21,22) and delaying task failure (18). The present study is the first to demonstrate that IPC can also slow the previously observed fatigue-induced loss of muscle torque complexity (6,9), suggesting that IPC can influence motor control. As fatigue developed, ApEn decreased (indicating increased signal regularity) and DFA α increased (indicating increasingly Brownian fluctuations in torque), with both metrics reaching the same level at task failure in each condition. However, the rate at which ApEn decreased and DFA α increased were significantly attenuated

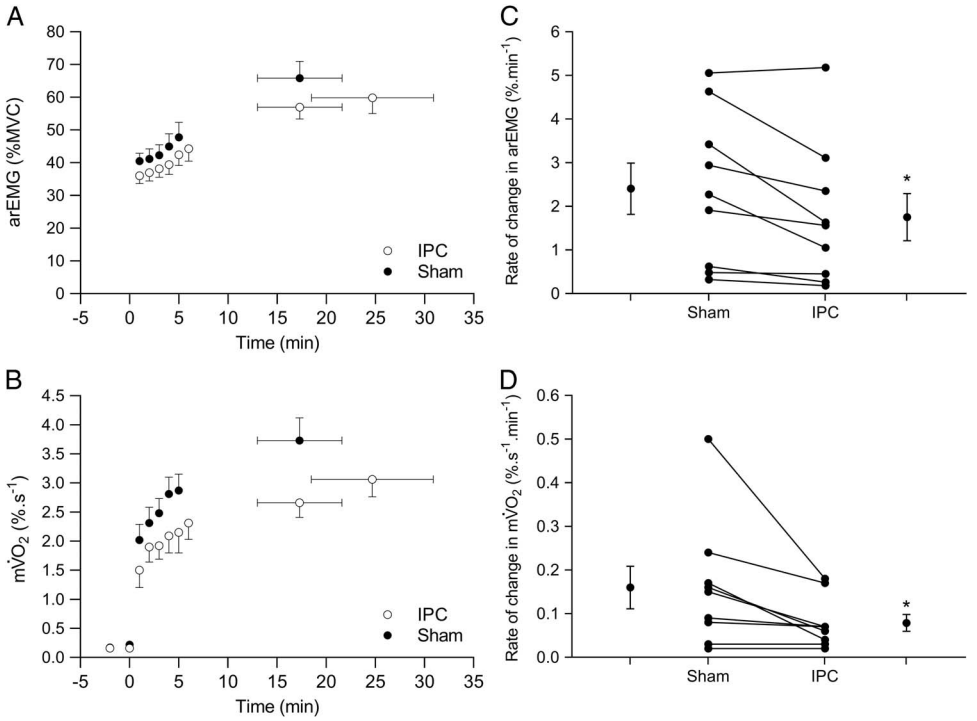

FIGURE 2—The arEMG (A) and the $m\dot{V}O_2$ (panel B) responses to contractions performed in the IPC (*black circles*) and SHAM (*white circles*) conditions, and the group and individual rates of change in EMG (C) and $m\dot{V}O_2$ (D). Note that the first values in panel B are resting measurements taken before and after IPC/SHAM treatment. Values are presented as mean ± SEM. *Significantly different from SHAM.

after IPC (Table 3; Fig. 3C and D). Furthermore, at isotime in the IPC condition, ApEn remained significantly higher than at task failure in the SHAM condition (Fig. 3A). Consequently, the complexity of neuromuscular output during fatiguing contractions was better maintained with prior IPC, which presumably preserved the adaptability of the neuromuscular system (5) and allowed the task to be sustained for a longer duration (10).

The increase in time to task failure and the slowing of the loss of muscle torque complexity after IPC were accompanied by a significant slowing in the rate of global fatigue development (i.e., the loss of MVC torque; Table 2) and in the rates of increase in both $m\dot{V}O_2$ and arEMG (Table 2; Fig. 1C and D, respectively). There was, however, no slowing in the rate of central fatigue development, a finding consistent with Halley et al. (29). Previous studies have implicated both alterations in EMG responses (20,24) and $\dot{V}O_2$ (14,24) in the ergogenic effect of IPC. The rise in $m\dot{V}O_2$ beyond the primary amplitude (i.e., first 2 min of exercise [31]) is likely the result of a slow component of the $m\dot{V}O_2$ response to high-intensity exercise (32). This slow component has been associated with the recruitment of additional motor units as exercise progresses (32), which is sometimes reflected in a greater arEMG amplitude (33). As such, these results imply that the requirement for additional motor unit recruitment as exercise progresses is reduced after IPC.

Physiological basis for change in torque complexity with IPC. Although the utility of IPC as an ergogenic aid has only been established within the last decade (14), it has quickly been demonstrated in a range of exercise tasks (15,16,18). The results of the present study demonstrated that IPC increased time to task failure of the knee extensors during submaximal intermittent isometric exercise by ~43% (Table 2). Although there is a growing body of evidence which suggests that IPC improves exercise performance, the mechanistic basis for this has remained elusive. Initially, enhanced oxygen delivery to working muscle was considered the most likely mechanism of

TABLE 3. Variability, complexity, and fractal scaling responses during contractions in the IPC and SHAM conditions.

Parameter	SHAM	IPC
SD		
SD at task beginning, N·m	2.0 ± 0.2	2.0 ± 0.2
SD at isotime, N·m	–	3.4 ± 0.6
SD at task failure, N·m	4.3 ± 0.4*	5.0 ± 0.7*
$\Delta SD/\Delta t$, N·m·min^{-1}	0.3 ± 0.1	0.3 ± 0.1
CV		
CV at task beginning, %	2.0 ± 0.2	2.0 ± 0.1
CV at isotime, %	–	3.4 ± 0.3
CV at task failure, %	5.0 ± 0.6*	5.6 ± 0.7*
$\Delta CV/\Delta t$, %·min^{-1}	0.4 ± 0.1	0.3 ± 0.1
ApEn		
ApEn at task beginning	0.44 ± 0.02	0.44 ± 0.02
ApEn at isotime	–	0.27 ± 0.04#
ApEn at task failure	0.14 ± 0.02*	0.16 ± 0.03*
$\Delta ApEn/\Delta t$	–0.04 ± 0.01	–0.02 ± 0.01#
DFA α		
DFA α at task beginning	1.33 ± 0.05	1.33 ± 0.05
DFA α at isotime	–	1.43 ± 0.06
DFA α at task failure	1.53 ± 0.05*	1.50 ± 0.06*
$\Delta DFA\ \alpha/\Delta t$	0.03 ± 0.01	0.02 ± 0.01#

Values are presented as mean ± SEM. Symbols indicate a statistically significant difference compared with the following: *Value at task beginning (2 min into exercise, to account for primary amplitude of $\dot{V}O_2$ response). #SHAM. Isotime in the IPC condition is compared with task failure in the SHAM condition.
CV, coefficient of variation; Δ, change; *t*, time.

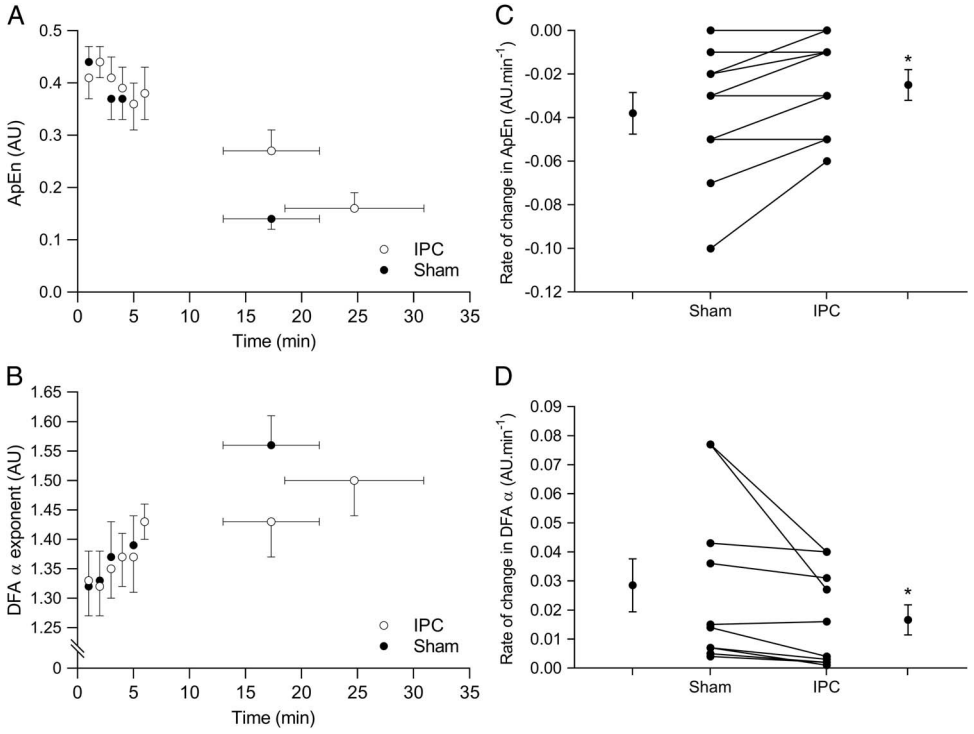

FIGURE 3—The ApEn (A) and the DFA α exponent (B) responses to contractions performed in the IPC (*black circles*) and SHAM (*white circles*) conditions, and the group and individual rates of change in ApEn (C) and DFA α (D). Values are presented as mean ± SEM. *Significantly different from SHAM.

the IPC-mediated performance improvement (14,34); however, recent evidence has suggested that changes in neural drive, as elucidated below, may be of greater importance (20,22).

IPC has previously been demonstrated to increase EMG amplitude during exhaustive exercise at peak aerobic power output, and during maximal sprints and maximal isometric contractions (22,24), and to decrease the force recruitment threshold of motor units during submaximal isometric contractions (22). These responses are consistent with increased excitability of the motoneuron pool (25). By contrast, the results of the present study show that the rate of increase in arEMG was slowed after IPC (Table 2; Fig. 2C). The progression of fatiguing submaximal contractions necessitates an increase in the excitatory drive to motoneurons, which leads to the more frequent activation of a larger number of motor units to maintain torque, with this response reflected in an increase in EMG activity (27). This results in increased energy demand and thus $m\dot{V}O_2$ during submaximal contractions, as illustrated by the slow component response (32). Our results demonstrated that the fatigue-induced rate of decrease in MVC torque was attenuated with IPC, implying that IPC reduces fatigability, which in turn reduces the requirement for additional motor unit recruitment and thus increased $m\dot{V}O_2$.

We have previously argued that changes in the ensemble behavior of the motor unit pool, specifically increases in common synaptic input, may be responsible for the fatigue-induced loss of muscle torque complexity (6,9). Common synaptic input has been postulated to be the main determinant of torque variability (35), based on the coherence between the cumulative motor unit spike train and the muscle torque output (36). Furthermore, common synaptic input to motoneurons has been demonstrated to increase when the net excitatory drive to motoneurons increases as a consequence of both changes in force and the development of neuromuscular fatigue (37). The presently observed IPC-mediated attenuation of the rate of fatigue development (i.e., slowing of the decrease in MVC torque and increases in arEMG and $m\dot{V}O_2$) therefore suggests a slowing in the fatigue-induced increase in common synaptic input (37). We have postulated that any increase in common synaptic input should be reflected in a decrease in muscle torque complexity (10). Thus, a slowing in the fatigue-induced increase in common synaptic input should result in a concomitant slowing in the decrease in muscle torque complexity. However, as previously noted (12), direct measurement of individual motor unit spike trains, using either high-density surface of intramuscular EMG (rather than the bipolar EMG used in the present study), is necessary to conclusively demonstrate a link between muscle torque complexity and common synaptic input.

Limitations. The present study was subject to some limitations. First, it was not possible to blind participants to the two experimental conditions, as they are aware of the significant pressure difference between the IPC and the SHAM conditions. This is, however, a limitation inherent to any study on IPC. To account for this, participants were informed that both IPC and SHAM might influence performance (21). Second, there are limitations associated with the estimation of $m\dot{V}O_2$ using NIRS. The penetration of the NIRS probe is approximately 1.5 cm, meaning that it detects changes in a small and relatively superficial volume of the vastus lateralis. Koga

et al. (38) demonstrated that the kinetics of [HHb] are not different at two different depths in the rectus femoris but are different from those of the vastus lateralis. Our estimation of $m\dot{V}O_2$ is therefore specific to the vastus lateralis and may not reflect the $m\dot{V}O_2$ of the other quadriceps muscles. Third, we were unable to identify the location of the neural effects of IPC. This could be achieved in the future through the use of further electrical stimulation techniques (i.e., H-reflexes), transcranial magnetic stimulation, and cervicomedullary stimulation. Finally, as mentioned above, the use of bipolar surface EMG does not allow the characterization of individual motor unit thresholds and firing rates, which previous studies have implicated in the fatigue-induced loss of muscle torque complexity (6,12) and IPC's effect on motor output (22). The use of high-density arrays and/or intramuscular EMG is required to confirm whether such changes in motor unit behavior are responsible for the loss of torque complexity and the ergogenic effect of IPC.

CONCLUSION

In summary, the present study has demonstrated that IPC increased time to task failure and slowed the fatigue-induced loss of muscle torque complexity, as measured using ApEn and DFA α, during submaximal intermittent isometric knee extensor exercise. IPC also attenuated the rates of increase in $m\dot{V}O_2$ and EMG amplitude. The loss of motor output complexity, and adaptability, therefore remains tightly coupled to the neuromuscular fatigue process and the greater activation of the motor unit pool this entails. These results further suggest a neural contribution to the loss of muscle torque complexity with neuromuscular fatigue and provide further evidence that IPC's ergogenic effect is mediated by neural mechanisms.

This work was supported by a research project grant from the Leverhulme Trust (RPG-2016-440) and a Summer Vacation Research prize from the University of Kent.

This work was completed at the University of Kent. J. P. conceived and designed the study. J. P. and C. C. collected the data. S. W. wrote the MATLAB code to process the data. All authors were involved in the analysis and interpretation of the data and contributed to the writing and critical revisions of the manuscript. All authors approved the final version of the manuscript.

The authors report no competing interests for this work. The results of the present study do not constitute endorsement by the American College of Sports Medicine. The results of the study are presented clearly, honestly, and without fabrication, falsification, or inappropriate data manipulation.

REFERENCES

1. Slifkin AB, Newell KM. Noise, information transmission, and force variability. *J Exp Psych*. 1999;25:837.
2. Contessa P, Adam A, De Luca CJ. Motor unit control and force fluctuation during fatigue. *J Appl Physiol*. 2009;107:235–43.
3. Galganski ME, Fuglevand AJ, Enoka RM. Reduced control of motor output in a human hand muscle of elderly subjects during submaximal contractions. *J Neurophysiol*. 1993;69:2108–15.
4. Goldberger AL, Amaral LA, Hausdorff JM, Ivanov PC, Peng CK, Stanley HE. Fractal dynamics in physiology: alterations with disease and aging. *PNAS*. 2002;99:2466–72.
5. Vaillancourt DE, Newell KM. Aging and the time and frequency structure of force output variability. *J Appl Physiol*. 2003;94:903–12.
6. Pethick J, Winter SL, Burnley M. Fatigue reduces the complexity of knee extensor torque fluctuations during maximal and submaximal intermittent isometric contractions in man. *J Physiol*. 2015;593:2085–96.
7. Pincus SM. Approximate entropy as a measure of system complexity. *PNAS*. 1991;88:2297–301.
8. Peng CK, Buldyrev SV, Havlin S, Simons M, Stanley HE, Goldberger AL. Mosaic organization of DNA nucleotides. *Phys Rev E*. 1994;49:1685–9.
9. Pethick J, Winter SL, Burnley M. Loss of knee extensor torque complexity during fatiguing isometric muscle contractions occurs exclusively above the critical torque. *Am J Physiol*. 2016;310:R1144–53.
10. Pethick J, Winter SL, Burnley M. Effects of ipsilateral and contralateral fatigue and muscle blood flow occlusion on the complexity of knee-extensor torque output in humans. *Exp Physiol*. 2018;103:956–67.
11. Pethick J, Winter SL, Burnley M. Relationship between muscle metabolic rate and muscle torque complexity during fatiguing intermittent isometric contractions in humans. *Phys Rep*. 2019;7:e14240.
12. Pethick J, Winter SL, Burnley M. Caffeine ingestion attenuates fatigue-induced loss of muscle torque complexity. *Med Sci Sports Exerc*. 2018;50:236–45.
13. Sharma V, Marsh R, Cunniffe B, Cardinale M, Yellon DM, Davidson SM. From protecting the heart to improving athletic performance—the benefits of local and remote ischaemic preconditioning. *Cardiovascr Drug Ther*. 2015;29:573–88.
14. De Groot PC, Thijssen DH, Sanchez M, Ellenkamp R, Hopman MT. Ischemic preconditioning improves maximal performance in humans. *Eur J Appl Physiol*. 2010;108:141–6.
15. Bailey TG, Jones H, Gregson W, Atkinson G, Cable NT, Thijssen DH. Effect of ischemic preconditioning on lactate accumulation and running performance. *Med Sci Sports Exerc*. 2012;44:2084–9.
16. Kilding AE, Sequeira GM, Wood MR. Effects of ischemic preconditioning on economy, VO_2 kinetics and cycling performance in endurance athletes. *Eur J Appl Physiol*. 2018;118:2541–9.
17. Barbosa TC, Machado AC, Braz ID, et al. Remote ischemic preconditioning delays fatigue development during handgrip exercise. *Scand J Med Sci Sport*. 2015;25:356–64.
18. Tanaka D, Suga T, Tanaka T, et al. Ischemic preconditioning enhances muscle endurance during sustained isometric exercise. *Int J Sports Med*. 2016;37:614–8.
19. Donato M, Buchholz B, Rodríguez M, et al. Role of the parasympathetic nervous system in cardioprotection by remote hindlimb ischaemic preconditioning. *Exp Physiol*. 2013;98:425–34.
20. Cruz RS, Pereira KL, Lisbôa FD, Caputo F. Could small-diameter muscle afferents be responsible for the ergogenic effect of limb ischemic preconditioning? *J Appl Physiol*. 2017;112:718–20.
21. Paradis-Deschênes P, Joanisse DR, Billaut F. Sex-specific impact of ischemic preconditioning on tissue oxygenation and maximal concentric force. *Front Physiol*. 2017;7:674.
22. Hyngstom AS, Murphy SA, Nguyen J, et al. Ischemic conditioning increases strength and volitional activation of paretic muscle in chronic stroke: a pilot study. *J Appl Physiol*. 2018;124:1140–7.
23. Phillips DJ, Petrie SG, Zhou BH, Guanche CA, Baratta RV. Myoelectric and mechanical changes elicited by ischemic preconditioning in the feline hindlimb. *J Electromyogra Kinesiol*. 1997;7:187–92.
24. Cruz RS, De Aguiar RA, Turnes T, Pereira KL, Caputo F. Effects of ischemic preconditioning on maximal constant-load cycling performance. *J Appl Physiol*. 2015;119:961–7.
25. Heckman CJ, Enoka RM. Motor unit. *Comp Physiol*. 2012;2:2629–82.

26. Taylor JL, Amann M, Duchateau J, Meeusen R, Rice CL. Neural contributions to muscle fatigue: from the brain to the muscle and back again. *Med Sci Sport Exerc*. 2016;48:2294–306.
27. Farina D, Merletti R, Enoka RM. The extraction of neural strategies from the surface EMG: an update. *J Appl Physiol*. 2014;117:1215–30.
28. Ryan TE, Erickson ML, Brizendine JT, Young HJ, McCully KK. Noninvasive evaluation of skeletal muscle mitochondrial capacity with near-infrared spectroscopy: correcting for blood volume changes. *J Appl Physiol*. 2012;113:175–83.
29. Halley SL, Marshall P, Siegler JC. The effect of ischaemic preconditioning on central and peripheral fatiguing mechanisms in humans following sustained maximal isometric exercise. *Exp Physiol*. 2018;103:976–84.
30. Behm DG, St-Pierre DM, Perez D. Muscle inactivation: assessment of interpolated twitch technique. *J Appl Physiol*. 1996;81:2267–73.
31. Burnley M, Jones AM. Oxygen uptake kinetics as a determinant of sports performance. *Eur J Sport Sci*. 2007;7:63–9.
32. Poole DC, Schaffartzik W, Knight DR, et al. Contribution of exercising legs to the slow component of oxygen uptake kinetics. *J Appl Physiol*. 1991;71:1245–60.
33. Shinohara M, Moritani T. Increase in neuromuscular activity and oxygen uptake during heavy exercise. *Ann Physiol Antropol*. 1992; 11:257–62.
34. Kido K, Suga T, Tanaka D, et al. Ischemic preconditioning accelerates muscle deoxygenation dynamics and enhances exercise endurance during the work-to-work test. *Phys Rep*. 2015;3:e12395.
35. Farina D, Negro F. Common synaptic input to motor neurons, motor unit synchronization and force control. *Ex Sport Sci Rev*. 2015;43: 23–33.
36. Negro F, Holobar A, Farina D. Fluctuations in isometric muscle force can be described by one linear projection of low-frequency components of motor unit discharge times. *J Physiol*. 2009;587:5925–38.
37. Castronovo AM, Negro F, Conforto S, Farina D. The proportion of common synaptic input to motor neurons increases with an increase in net excitatory input. *J Appl Physiol*. 2015;119:1337–46.
38. Koga S, Okushima D, Barstow TJ, Rossiter HB, Kondo N, Poole SC. Near-infrared spectroscopy of superficial and deep rectus femoris reveals markedly different exercise response to superficial vastus lateralis. *Phys Rep*. 2017;5:e13402.